

with relatively small dispersive features. In contrast, the type I configuration produces a larger, more symmetric error signal, especially at the crossover. We therefore restrict the rest of discussion to the type I crossover. The relative prominence of the crossover suggests that hyperfine pumping plays a significant role [16]. To see this, consider atoms with zero velocity along the optical axis, for which the pump and probe are at the same frequency and therefore address the same hyperfine ground state. Then hyperfine pumping results in a transfer of population into the other ground state, which is out of resonance with the probe. In contrast, for ground state crossovers, this process increases the population interacting with the probe (recall the enhanced CO absorption in Fig. 1).

To understand the basic physics of the Type I spectroscopy in more detail, we consider a pair of simple two-level systems, each corresponding to one of the pump-probe pairs. For a probe below the saturation intensity, the signal at each photodiode is proportional to $\exp(-\alpha)$, where α is the relevant absorption coefficient. In our configuration, the two probes experience absorption coefficients [2]

$$\alpha_{\pm} = \alpha_{D\pm}(1 - \mathcal{L}_{\pm}) \quad (2)$$

where $\alpha_{D\pm}$ are the Doppler-broadened absorption coefficients, and $\mathcal{L}_{\pm} = A_{\pm}/[1 + (x \pm \delta)^2]$ are sub-Doppler Lorentzians whose amplitudes A_{\pm} and widths generally depend on the pump and probe intensities. As above x is the detuning normalized to the broadened width; δ is the Zeeman shift similarly normalized. For small α_{\pm} the difference signal is

$$\Delta V \approx \alpha_{-} - \alpha_{+} \quad (3)$$

The amplitude $A_{+} = A_{-}$ by symmetry. The Zeeman shift is on the order of Γ which is much smaller than the Doppler width Δ . In this case $\alpha_{D+} \approx \alpha_{D-}$, and we can write

$$\Delta V = A \left[\frac{1}{1 + (x - \delta)^2} - \frac{1}{1 + (x + \delta)^2} \right] \quad (4)$$

For small applied magnetic fields, the signal is thus approximately proportional to the derivative of a Lorentzian [7].

From Eq. (4) the slope at the lock point is $4A\delta/(1 + \delta^2)^2$, which grows linearly with small δ and has a maximum for $\delta_0 = 3^{-1/2} \approx 0.6$. It is possible to obtain a closed expression for the capture range, defined by the peak-to-peak width of the error signal, as well as the signal amplitude. However the expressions are complicated and not very enlightening. In the regime of interest ($\delta < 1$), the predicted capture range is approximately constant for small fields and only grows by 25% by δ_0 . In contrast, the error signal amplitude grows linearly for small δ and then saturates when the \pm peaks fully separate.

Figure 7 shows the observed dependence of the crossover error signal on magnetic field. Despite the complexity of the real atomic system, the behavior is qualitatively as expected from the two-level model. We observe a small feature even at zero applied field, which we attribute to the residual ambient field and imperfect light polarization. The optimum slope is obtained at ~ 14 G. In the limit of perfect optical pumping into large- $|m_F|$ states, the crossover should be dominated by the $(F, |m_F|) = 1 \rightarrow (F', |m'_F|) = 2$ and $(F, |m_F|) = 2 \rightarrow (F', |m'_F|) = 3$ transitions, which have the greatest oscillator strengths [20]. In a magnetic field B , the resonances are Zeeman shifted in energy by $(g'_F m'_F - g_F m_F) \mu_B B$, where $\mu_B \approx 9.28 \times 10^{-28}$ J/G is the electron magnetic moment and g_F is the hyperfine Landé g -factor. For the ground states $g_1 = -1/2$ and $g_2 = 1/2$, and for the excited states $g'_2 = 2/3 = g'_3$. The optimum field thus corresponds to shifts of 19 MHz and 35 MHz for the $2 - 3'$ and $1 - 2'$ transitions, respectively. Although this is much larger than the natural line width $\gamma/(2\pi)$, our saturated absorption crossovers are typically ~ 20 MHz wide [12].

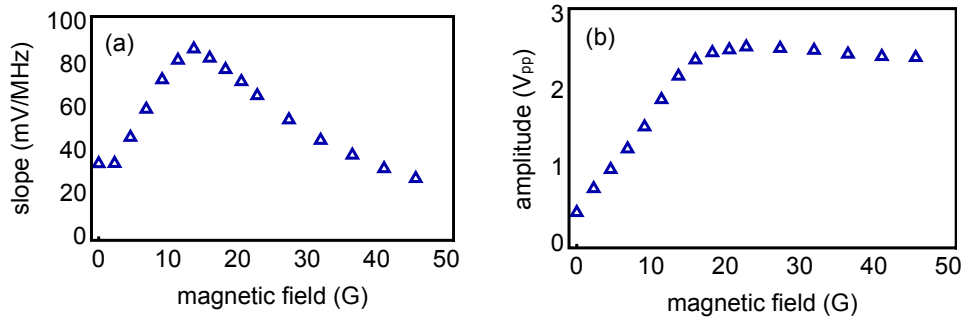


Fig. 7. Dependence of the magnetic dichroism error signal with applied field. Only data for the crossover are shown. The pump intensities were 2.7 ± 0.5 mW/cm² each, measured just before the cell. (a) Slope at the zero-crossing. (b) Peak-to-peak amplitude.

In Fig. 8 we show the dependence of the error signal on beam intensity. Note that since we retroreflect our pump beams, both pump and probe beam intensities are varying together. Above I_{sat} the amplitude and slope are essentially linear over the whole range of intensities we have tried. The lack of saturation and the constant ratio of amplitude to width suggests there is little or no broadening, even at intensities well above I_{sat} .

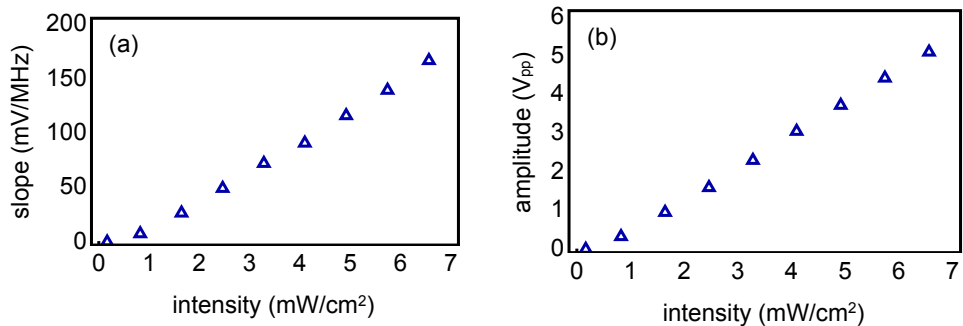


Fig. 8. Dependence of the MD error signal on beam intensity. Shown is the intensity per pump beam, measured just before the cell. The magnetic field was 10.3 G. (a) Slope at the zero-crossing. (b) Peak-to-peak amplitude.

4. Discussion

We have studied polarization spectroscopy (PS) and magnetic dichroism (MD) for laser frequency stabilization near the potassium D₂ transitions at 767 nm. These methods produce dispersive error signals which are roughly linear in detuning around a zero-voltage locking point. The main practical difference between the two methods is that the PS signal is best suited for locking near the $F = 2$ feature, while the MD signal favors the crossover. This reflects the general strength of PS lines at cycling transitions, whereas MD spectroscopy can be used for nearly any strong absorptive feature; this distinction was noted in the case of rubidium in [14]. The preferred lock point depends on the details of the experiment, such as which isotope is under study, the desired detuning from resonance, and whether or not frequency shifting elements such as acousto-optic modulators are to be used.

As described in [12], a critical parameter for laser locking is the error signal slope. This rep-

resents a gain term within the total stabilization loop which is not constrained by limitations such as the fixed gain-bandwidth product typical of electronic components. In this sense, our modified MD signal appears to be superior to PS, giving a $\sim 2\times$ greater slope. However, after preparing this manuscript, we became aware of a type of polarization spectroscopy using a split-beam configuration similar to that used in our MD experiments [21]. Such a modification might also increase the slope of our PS signal. Other figures of merit include the signal amplitude and the capture range, which we take to be the peak-to-peak width. The PS capture range is slightly larger, but the MD signal amplitude is $4\times$ greater. In turn, the PS noise level was typically 7 mV (root-mean-squared), compared to 20 mV for MD. Both methods tolerate relatively high intensities, with MD especially insensitive. Although similar work with rubidium MD spectroscopy showed an optimum intensity [14], we were not able to reach high enough laser powers to see a roll-over in our setup.

Although our system has not been in operation long enough to acquire information on long-term stability, our previous experience with rubidium suggests that both methods will be sensitive to temperature-dependent drifts in polarization. Furthermore, this experience suggests that the lock point does not occur exactly at resonance, but can be as much as 10 MHz off-resonance. We do not yet know if this offset is stable over time, but we expect it to similarly drift with polarization and vapor pressure (through the cell temperature). One possible advantage of magnetic dichroism may be with respect to B -field sensitivity. Polarization spectroscopy is typically performed at zero or low bias field (we used 20 mG), whereas MD was optimized with 14 G. We therefore expect MD spectroscopy to be more robust to changes in ambient field.

Table 1. Comparison of modulation-based and modulation-free error signals. Results for direct modulation (DM) and modulation transfer (MT) are from [12]. Numbers for MD correspond to the crossover, and all others to the $F = 2$ feature.

| Method | Slope | Amplitude | Capture Range | Noise | Bandwidth |
|--------|-----------|---------------------|---------------|---------------------|-----------|
| PS | 80 mV/MHz | 1.2 V _{pp} | 56 MHz | 7 mV _{rms} | 750 kHz |
| MD | 170 | 5.1 | 36 | 20 | 750 |
| DM | 100 | 0.4 | 15 | 15 | 200 |
| MT | 600 | 1.3 | 5 | 15 | 200 |

Finally, we compare our PS and MD results with our previous results using heterodyne spectroscopy. In [12] we performed modulation spectroscopy either by direct phase modulation of the probe (DM) or by non-linear modulation transfer from the pump (MT). The results are summarized in Table 1. The modulation-free methods presented here compare well with direct modulation, and use only standard optics available in most labs. Modulation transfer is unique in both its high slope (600 mV/MHz) and narrow capture range (5 MHz). This could be an advantage for experiments requiring a tight lock with relatively little error or drift in the lock-point. However the exceedingly narrow capture range could cause the laser to lose its lock in noisy environments.

Acknowledgments

This work was funded by EPSRC (EP/E036473/1). We acknowledge useful discussions with members of the Cold Atoms group at the University of Birmingham. We are grateful to V. Boyer for pointing out the role of four-level ground-state crossovers, and to P. Petrov and Y. Singh for carefully reading the manuscript.